Available online at www.sciencedirect.com
SCIENCE DIRECT®
Bioorganic & Medicinal Chemistry Letters 16 (2006) 262–266
Bioorganic & Medicinal Chemistry Letters

Pyrazoloheteroaryls: Novel p38α MAP kinase inhibiting scaffolds with oral activity

Laszlo Revesz,* Ernst Blum, Franco E. Di Padova, Thomas Buhl, Roland Feifel, Hermann Gram, Peter Hiestand, Ute Manning, Ulf Neumann and Gerard Rucklin

Novartis Institutes for BioMedical Research, Global Discovery Chemistry, CH-4002 Basel, Switzerland

Received 13 July 2005; revised 30 September 2005; accepted 5 October 2005
Available online 24 October 2005

Abstract—A test library with three novel p38α inhibitory scaffolds and a narrow set of substituents was prepared. Appropriate combination of substituent and scaffold generated potent p38α inhibitors, for example, pyrazolo[3,4-*b*]pyridine **9**, pyrazolo[3,4-*d*]pyrimidine **18a** and pyrazolo[3,4-*b*]pyrazine **23b** with potent in vivo activity upon oral administration in animal models of rheumatoid arthritis.
© 2005 Elsevier Ltd. All rights reserved.

Inhibition of p38α has become one of the major targets in developing anti-inflammatory drugs, which is due to its prominent role in regulating inflammatory cytokines such as TNFα and IL-1.[1] The benefits of treating rheumatoid arthritis patients with TNFα inhibitors (Enbrel® and Remicade®) or IL-1 inhibitors (Kineret®) have raised the desire to develop oral treatments. Blockade of p38α is a very attractive option: p38α inhibitors downregulate production and signalling of TNFα, IL-1 and in addition inhibit COX-2 induction. The value of COX-2 inhibitors (Celebrex®, Vioxx®) has been proved by their use in arthritic diseases.

Since the discovery of pyridinylimidazoles,[2] several novel structural classes of p38 inhibitors have been reported.[3] Our search for p38 inhibitors unrelated to pyridinylimidazoles resulted in pyrido[2,3-*d*]pyrimidine **1**, a modest p38α inhibitor (IC_{50} = 5.8 μM), while its ring opened analogue **2** was 10 times more potent.

Further modifications gave rise to benzoylpyridines, benzophenones[4] and the pyrazoloheteroaryls **3**–**5**, some with subnanomolar IC_{50}s. Here, we wish to report on the in vitro and in vivo SAR of pyrazolo[3,4-*b*]pyridines **3**, pyrazolo[3,4-*d*]pyrimidines **4** and pyrazolo[3,4-*b*]pyrazines **5**, three novel p38α inhibiting scaffolds. A narrow set of substituents R was chosen, aiming at potential interactions with Asp164.

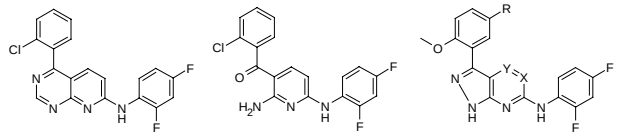

The synthesis of pyrazolo[3,4-*b*]pyridines **9**–**14** is described in Schemes 1 and 2. 2,6-Dichloro-3-lithiopyridine (Scheme 1) reacted with 5-bromo-2-methoxybenzaldehyde to provide the alcohol, which upon Jones[5] oxidation gave ketone **6**. The latter was treated with hydrazine and furnished pyrazolo[3,4-*b*]pyridine **7**. Sonogashira[6] coupling conditions were applied to attach the 1,1-dimethylpropynylamine side chain in **8**, followed by a Buchwald[7] reaction to substitute the Cl-atom by 2,4-difluoroaniline in **9**. Hydrogenation yielded the saturated analogue **10**.

Synthesis of pyrazolo[3,4-*b*]pyridines **13a**–**c** and **14a**,**b** (Scheme 1) started by SEM protection of **7**, followed by Br–Li exchange and CO_2 treatment to render acid **11**. 2,4-Difluoroaniline was introduced under Buchwald[7] conditions to provide **12a**, which was first coupled with 4-aminotetrahydropyran, cyclopentylamine and

Keywords: p38 inhibition; MAP kinase inhibition; Rheumatoid arthritis; Antiarthritic; Anti-inflammatory; Collagen-induced arthritis; Adjuvant-induced arthritis.
* Corresponding author. Tel.: +41 61 324 3231; fax: +41 61 324 3273; e-mail: laszlo.revesz@novartis.com

0960-894X/$ - see front matter © 2005 Elsevier Ltd. All rights reserved.
doi:10.1016/j.bmcl.2005.10.015

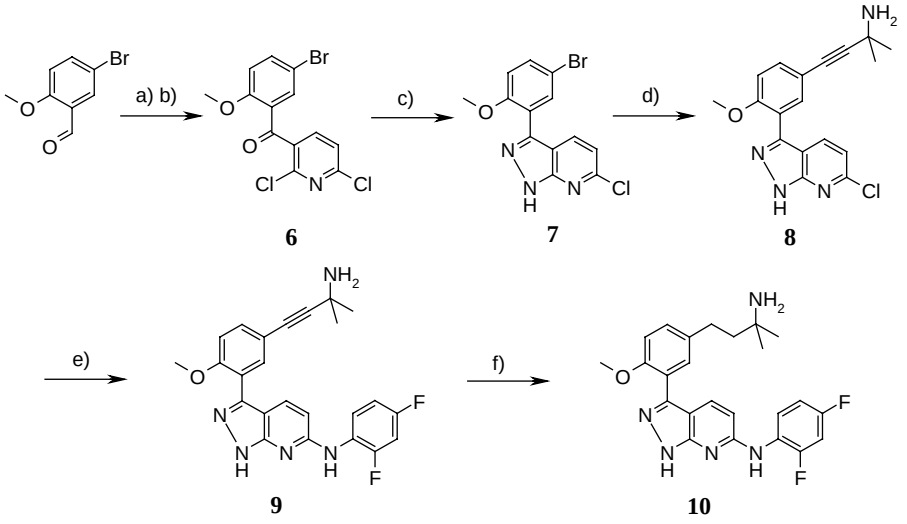

Scheme 1. Reagents and conditions: (a) 2,6-Dichloropyridine, LDA, −78 °C, 80%. (b) CrO_3, H_2SO_4, acetone, water, 79%. (c) $H_2NNH_2 \cdot H_2O$, EtOH/1-BuOH (1:1) reflux, 1 h, 70%. (d) $PdCl_2(PPh_3)_2$, CuI, Cs_2CO_3, 1,1-dimethylpropynylamine, reflux in DIPEA, 39%. (e) $Pd(OAc)_2$, Cs_2CO_3, *R*-(+)-BINAP, 2,4-difluoroaniline, 1,4-dioxane, reflux 2 h, 22%. (f) EtOH, Pd/C, H_2, 30 min, 85%.

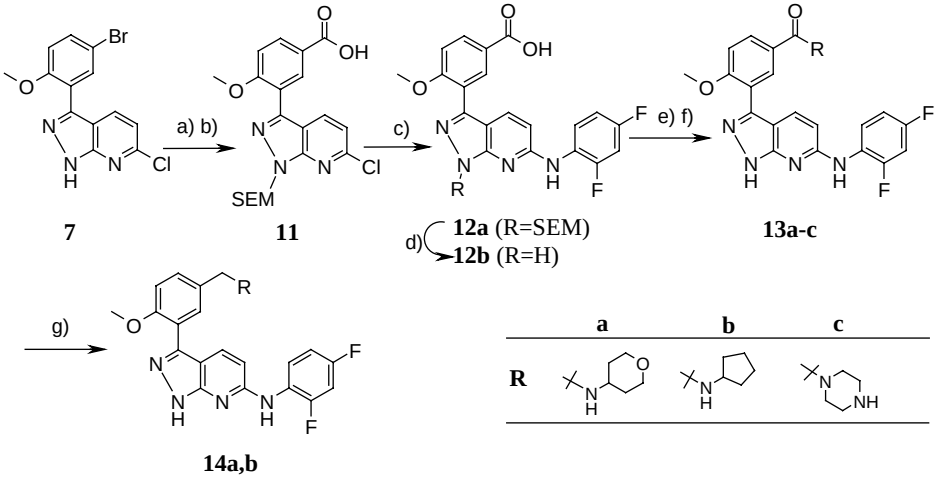

Scheme 2. Reagents and conditions: (a) $KN(TMS)_2$, SEM-Cl, THF, −78 °C, 72% (2 regioisomers). (b) *n*-BuLi, −78 °C, THF, CO_2, 63%. (c) $Pd(OAc)_2$, PPh_3, NaOtBu, *R*-(+)-BINAP, 2,4-difluoroaniline, 1,4-dioxane, reflux 15 min, 96%. (d) EtOH, HCl concn 1:1, 2 min, 60 °C, 50%. (e) 1,1′-Carbonyldiimidazole, amine, THF, reflux 10 min, 60–80%. (f) **13a**–**c**: EtOH, HCl concn 1:1, 15 min, 60–70%. (g) DIBAL-H, THF, reflux, 10 min, 70%.

1-Boc-piperazine and then deprotected to deliver amides **13a-c**. DIBAL-H reduction yielded amines **14a** and **14b**.

Pyrazolo[3,4-*d*]pyrimidines **18** and **19** (Scheme 3) were prepared by reacting 5-lithio-2,4-dichloropyrimidine with 5-bromo-2-methoxybenzaldehyde and oxidising the resulting alcohol to ketone **15**. Hydrazine at low temperature converted **15** into pyrazolo[3,4-*d*]pyrimidine **16**, which—combined for 15 min with 2,4-difluoroaniline at 150 °C—gave **17** in high yield. Sonogashira[6] coupling of **17** with a series of alkynes afforded **18a**–**d** in moderate yields. Hydrogenation gave rise to the saturated analogues **19a**–**d**.

Pyrazolo[3,4-*b*]pyrazines **23a**,**b** and **24a**,**b** were prepared (Scheme 4) by combining 2,6-dichloro-3-lithiopyrazine at −90 °C with 5-bromo-2-methoxybenzaldehyde. Jones[5] oxidation of the resulting alcohol delivered ketone **20**, which upon treatment with hydrazine furnished pyrazolo[3,4-*b*]pyrazine **21**. The remaining Cl-atom in **21** was substituted by 2,4-difluoroaniline by heating to 175 °C, giving rise to **22**; Sonogashira[6] coupling introduced the propargyl side chain in **23a**,**b**. Hydrogenation of the triple bond gave **24a**,**b**.

The 1,1-dimethylpropynylamino group common to pyrazolo[3,4-*b*]pyridine **9**, pyrazolo[3,4-*d*]pyrimidine **18a** and pyrazolo[3,4-*b*]pyrazine **23a** (IC_{50}s = 20, 12 and 10 nM) permitted us to compare the p38α inhibiting efficacies of the three pyrazoloheteroaryl scaffolds (Table 1). The inhibitory potencies of the three scaffolds proved to be very similar, with the tendency of the pyrazolo[3,4-*b*]pyrazine analogues to be slightly superior to those of pyrazolopyrimidines and pyrazolopyridines. An interac-

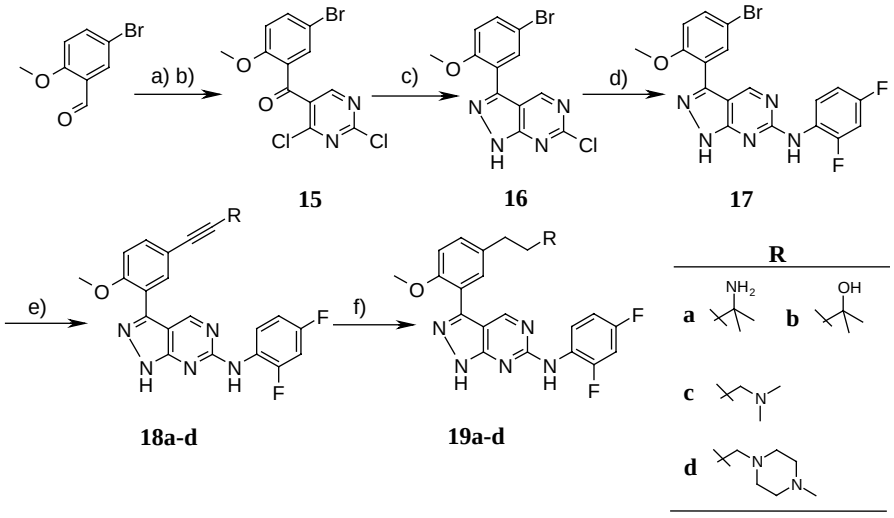

Scheme 3. Reagents and conditions: (a) 2,4-Dichloropyrimidine, LDA, −78 °C, 34%. (b) CrO_3, H_2SO_4, acetone, water, 88%. (c) $H_2NNH_2 \cdot H_2O$ (2 equiv), MeOH, −50 to 0 °C, 67%. (d) 2,4-Difluoroaniline (solvent), 15 min, 150 °C, 90%. (e) **18a**: $PdCl_2(PPh_3)_2$, CuI, Cs_2CO_3, 1,1-dimethylpropynylamine (10 equiv), DIPEA, autoclave, 130 °C, 1 h, 30%. **18b**: $PdCl_2(PPh_3)_2$, CuI, NEt_3, DMF, 1,1-dimethylpropynol (4 equiv), 1 h, 100 °C, 52%. **18c**: $Pd(OAc)_2$, *R*-(+)-BINAP, CuI, PPh_3, NaOtBu, diglyme, *N*,*N*-dimethylamino-2-propyne, autoclave, 1 h, 135 °C, 65%. **18d**: $Pd(OAc)_2$, *R*-(+)-BINAP, CuI, PPh_3, NaOtBu, 1-methyl-4-prop-2-ynylpiperazine, diglyme, 40 min, 145 °C, 75%. (f) EtOH, Pd/C, H_2, 1 h, 55–80%.

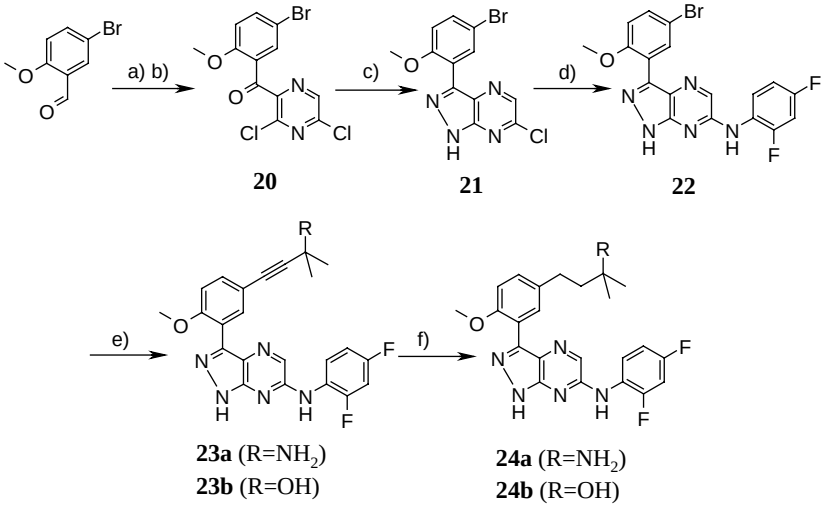

Scheme 4. Reagents and conditions: (a) LiTMP, −90 °C, 2,6-dichloropyrazine, 38%. (b) CrO_3, H_2SO_4, acetone, water, 88%. (c) $H_2NNH_2 \cdot H_2O$ (2 equiv), MeOH, 30 min, rt, 36%. (d) 2,4-Difluoroaniline, 1 h, 175 °C, 91%. (e) **23a**: $Pd(OAc)_2$, *R*-(+)-BINAP, CuI, NaOtBu, 1,1-dimethylpropynylamine, 1 h, 140 °C, 35%. **23b**: $PdCl_2(PPh_3)_2$, CuI, NEt_3, 1,1-dimethylpropynol, 1.5 h, 85 °C, 50%. (f) EtOH, Pd/C, H_2, 1 h, 70%.

tion of the 1,1-dimethylpropynylamino group of **9**, **18a** and **23a** with Asp164 seemed unlikely, since 1,1-dimethyl propynols **18b** and **23b** had similar potencies against p38α (IC_{50}s = 19, 7 nM). The saturated 1,1-dimethylpropylamines **10**, **19a** and **24a** (IC_{50}s = 33, 43 and 29 nM) and 1,1-dimethylpropanols **19b**, **24b** (IC_{50}s = 47 and 21 nM) were weaker than their propynyl precursors **9**, **18a**,**b** and **23a**,**b**, underlying the preference of rigid substituents for high affinity. Acid **12b** was not favoured, nor its piperazine amide **13c**. However, primary amides **13a** and **13b** were potent p38α inhibitors (IC_{50}s = 0.7 and 5 nM). Compared to the unsubstituted pyrazolo[3,4-*b*]pyridine (R = H; not shown in Table 1), **13a** was 100-fold more potent, revealing the important contribution of R to p38α inhibition. The reduced analogues **14a** and **14b** were considerably weaker than **13a** (IC_{50}s = 94 and 58 nM), demonstrating again the negative influence of increasing conformational freedom in the side chain on p38α inhibition. With the *N*,*N*-dimethylamino-2-propyne side chain in **18c** and its piperazine analogue **18d**, two further substituents with subnanomolar potency were identified (IC_{50}s = 0.6 and 0.9 nM). One may speculate that their basic amines interact favourably with the acidic Asp168 of p38α.[8] As expected, the saturated analogues **19c** and **19d** showed higher IC_{50}s (11 and 14 nM). The 7-fold difference between **13a** and **13b** may de due to a unique water-mediated hydrogen bond interaction of the pyran ring oxygen with Asp168.

With the exception of acid **12b**, all compounds underwent an in vivo screen for oral efficacy in the acute

Table 1. Inhibition of p38α and LPS-induced TNFα release in mice

Compound	p38α[a]	TNFα[b]
Pyrazolo[3,4-b]pyridine		
9	20	98
10	33	78
12b	200	n.t.
13a	0.7	97
13b	5	97
13c	280	3
14a	94	80
14b	58	38
Pyrazolo[3,4-d]pyrimidine		
18a	12	85
18b	19	98
18c	0.6	96
18d	0.9	96
19a	43	68
19b	47	98
19c	11	93
19d	14	73
Pyrazolo[3,4-b]pyrazine		
23a	10	98
23b	7	98
24a	29	0
24b	21	94

n.t., not tested.
[a] IC_{50} (nM).[10]
[b] % inhibition of LPS-induced TNFα release in mice at 20 mg/kg po.[9]

LPS-induced TNFα release in the mouse[9] at a standard dose of 20 mg/kg po (Table 1). Most compounds potently inhibited the release of TNFα.

Selected compounds with TNFα inhibition >80% were further tested in the subchronic adjuvant-induced arthritis (AIA)[11] model in the rat at 25 mg/kg po b.i.d. (Table 2). In the pyrazolo[3,4-*b*]pyridine series, the 1,1-dimethylpropynylamine and the 4-aminopyranylmethyl analogues **9** and **14a** showed appreciable activities with >45% inhibition of paw swelling. In spite of their high potency against p38α, both amides **13a** and **13b** were weak in AIA, possibly due to their short half-lives (1.4 and 1.6 h), low plasma concentrations (C_{max} = 6 nM at 1 mg/kg po) and modest bioavailabilities (BAV = 22% and 26%). In contrast to its 1,1-dimethylpropynylamine analogue **9** (BAV = 95%; C_{max} = 52 nM), the saturated 1,1-dimethylpropylamine **10** showed low BAV (20%), low plasma levels (C_{max} = 11 nM) and was inactive in AIA. In the pyrazolo[3,4-*d*]pyrimidine series, the 1,1-dimethylpropynylamine substituted **18a** showed the highest efficacy in AIA (69% inhibition of swelling). The closely related 1,1-dimethylpropynol substituted pyrazolo[3,4-*d*]pyrimidine **18b** and its saturated analogue **19b** were weaker. In the pyrazolo[3,4-*b*]pyrazine series, the 1,1-dimethylpropynylamine substituted **23a** and its alcohol analogue **23b** were nearly equipotent inhibitors of AIA, in spite of the low oral BAV (9%) and short half-life (2.6 h) of **23a**.

Table 2. Effects on adjuvant- and collagen-induced arthritis in rats

Compound	AIA[a]	CIA[b]
Pyrazolo[3,4-b]pyridine		
9	49	85
10	9	n.t.
13a	28	n.t.
13b	34	n.t.
14a	46	10
Pyrazolo[3,4-d]pyrimidine		
18a	69	75
18b	34	n.t.
19b	36	n.t.
Pyrazolo[3,4-b]pyrazine		
23a	37	n.t.
23b	41	57

[a] AIA[11]: adjuvant-induced arthritis in rats at 25 mg/kg po b.i.d.; % inhibition of swelling.
[b] CIA[13]: collagen-induced arthritis in rats at 10 mg/kg po q.d.; % inhibition of swelling.

Compound **23b** demonstrated an improved BAV (22%) and higher plasma levels (C_{max}: 160 nM at 1 mg/kg po). From the SAR above one may conclude that the side chains determine the degree of p38α inhibition, but that the in vivo potency with a given substituent is scaffold-dependent. For example, the three pyrazoloheteroaryls **9**, **18a** and **23a**—sharing the same 1,1-dimethylpropynylamine substituent—had similar potencies on p38α, but largely differed in oral BAV (95%, 16% and 9%). The potent in vivo effects of **18a** appear to be in contrast to its modest BAV, but can be explained by its high AUC.[12] In order to confirm AIA results in a different disease model, **9**, **14a**, **18a** and **23b** were tested in the collagen-induced arthritis (CIA)[13] model in rats. Compounds **9**, **18a** and **23b** showed potent inhibition of swelling in CIA (Table 2). Compounds **9** and **23b** were >1000-fold, **18a** >100-fold selective against a panel of 13 kinases.[14] No adverse inhibition of cytochrome P450 isoenzymes was observed.

Work is in progress to characterise, synthesize and optimise further analogues of the three novel p38α inhibitory scaffolds.

Acknowledgment

The kinase screening data by the Novartis oncology group are gratefully acknowledged.

References and notes

1. Chakravarty, S.; Dugar, S. *Annu. Rep. Med. Chem.* **2002**, *37*, 177.
2. Jackson, P. F.; Bullington, J. L. *Curr. Top. Med. Chem.* **2002**, *2*, 1011.
3. Cirillo, P. F.; Pargellis, C.; Regan, J. *Curr. Top. Med. Chem.* **2002**, *2*, 1021; Dominguez, C.; Powers, D. A.; Tamayo, N. *Curr. Opin. Drug Disc. Dev.* **2005**, *8*, 421.
4. Revesz, L.; Blum, E.; Di Padova, F. E.; Buhl, T.; Feifel, R.; Gram, H.; Hiestand, P.; Manning, U.; Rucklin, G. *Bioorg. Med. Chem. Lett.* **2004**, *14*, 3601.

5. Bowden, K.; Heilbron, I. M.; Jones, E. R. H.; Weedon, B. C. L. *J. Chem. Soc.* **1946**, *39*.
6. Sonogashira, K.; Tohda, Y.; Hagihara, N. *Tetrahedron Lett.* **1975**, *15*, 4467.
7. Muci, A. R.; Buchwald, S. L. *Top. Curr. Chem.* **2002**, *219*, 131.
8. Proposed binding mode of **18c** to p38α:

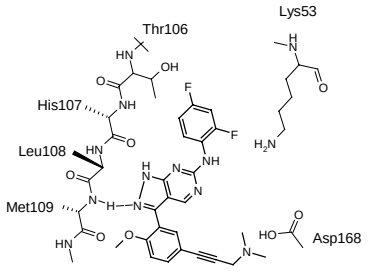

The proposed binding mode of pyrazoloheteroaryls to p38α implies that the pyrazolo nitrogen forms a crucial H-bridge to the NH of Met109 and the difluorophenyl ring accommodates in the specificity pocket near Thr106. Rigid basic substituents such as the 1-dimethylamino-2-propyne side chain in **18c** increase binding affinity by forming a salt bridge to Asp168.
9. Eight-week-old female OF1 mice were dosed orally by gavage with solutions of the compounds in DMSO/cornoil. One hour after dosing, LPS (20 mg/kg) was injected iv for stimulation of TNF-α release into plasma. One hour later blood was collected and TNF-α was determined using a mouse-specific ELISA.
10. A phosphorylated form of His-p38α MAP kinase (10 ng/well) of murine origin was used and immobilised GST-ATF-2 as substrate in the presence of 120 μM cold ATP.
11. AIA: Adjuvant-induced arthritis. Female Wistar rats were immunized with *Mycobacterium tuberculosis* at day 0 and dosed with the compounds (2×25 mg/kg po per day) from day 14 to 20. Swelling of the joints was measured on day 20.
12. The area under the curve (AUC) for **18a**: 512 [ng h ml^{-1}]; **9**: 422 [ng h ml^{-1}].
13. CIA: Collagen-induced arthritis. Female (WAGxBUF/F1) rats were immunized intradermally with bovine nasal septum type II collagen emulsified in Freund's incomplete adjuvant. Swelling started ~10 days after immunization. Dosing of compounds started on day 13, when swelling was nearly maximal. Compounds were dosed po once (q.d.) daily for 10 days.
14. Selectivity profiles were determined in-house as described.[4] Kinase (IC_{50} or % inhibition at 10 μM for **9**/**18a**/**23b**): JNK2 (100 μM/8.3 μM/>100 μM); CDK1: (0%/−16%/−13%); HER-1 (−43%/5.2 μM/0%); c-Abl (−23%/−58%/−42%); c-Src (−17%/−68%/−37%); Kdr (−12%/−55%/−12%); c-Met (−38%/1.5 μM/−17%); FGFR (−27%/10 μM/−5%); c-Kit (−31%/−37%/0%); IGF1R (0%/0%/−23%); HER-2 (−45%/5.0 μM/−0%); and c-Raf (n.t./0%/−14%).